Front. Chem. Sci. Eng. 2018, 12(1): 77–82
https://doi.org/10.1007/s11705-017-1684-5

RESEARCH ARTICLE

High-precision diffusion measurement of ethane and propane over SAPO-34 zeolites for methanol-to-olefin process

Dali Cai*, Yu Cui*, Zhao Jia, Yao Wang, Fei Wei (✉)

Beijing Key Laboratory of Green Reaction Engineering and Technology, Department of Chemical Engineering, Tsinghua University, Beijing 100084, China

Abstract The methanol-to-olefin (MTO) process has attracted much attention and many problems including lifetime and selectivity of light olefins have all been connected to the diffusion problems in zeolite crystals. However, a quantitative study of diffusion problems in SAPO-34 zeolites is lacking. In this paper, we performed a high-precision diffusion measurement of the diffusion behavior of ethane and propane, which represent ethylene and propylene respectively, over SAPO-34. The diffusions of ethane and propane over fresh and coked SAPO-34 zeolites with different crystal sizes were carefully studied. Ethane and propane show different diffusion behavior in SAPO-34. The diffusion of ethane is almost not influenced by the crystal size and coke percentage, whereas that of propane is strongly affected. A slower diffusion velocity was observed in bigger crystals, and the diffusion velocity decline significantly with the coke percentage increasing. The diffusion coefficient was calculated with both the internal and surface diffusion models, and the results show that the surface diffusion plays a key role in the diffusion process of both ethane and propane. We believe that this work would be helpful for understanding the diffusion of different molecules in SAPO-34 zeolites, and may lay the foundation of MTO research.

Keywords diffusion measurement, methanol-to-olefin process

1 Introduction

In recent years, the methanol-to-olefin (MTO) process has become attracted due to its competitive cost in producing ethylene and propylene in China [1−9]. Among the catalysts used in this process, one of the silicoaluminophosphate molecular sieves, marked as SAPO-34, is an efficient one for its suitable channel size [10−15]. Its smaller pore opening than other zeolites like ZSM-5 leads to a higher selectivity of lower olefins [16−19,6], but its smaller pore also leads to the diffusion difficulty [20−23], which is strongly related to its crystal size. A bigger crystal size may result in a higher diffusion resistance and a higher probability of secondary reactions such as hydrogen transfer reactions and coke deposition reactions. Under this consideration, a detailed measurement of the diffusion of different molecules is essential to MTO study and industrial application. To the best of our knowledge, however, a detailed quantitative study of the diffusion behavior in the SAPO-34 system is lacking [20]. Herein, we present a high accuracy diffusion test for the SAPO-34 system to determine quantitatively the influence of crystal size on diffusion resistance. It is difficult to measure directly the diffusion of ethylene and propylene because they tend to react in zeolite even at room temperature. Therefore, ethane and propane were selected to replace ethylene and propylene, respectively, for their similar molecular size and lower reactivity, though the diffusion of propylene and propane might be different due to the potential separation effect of 8-membered rings [24,25].

Received June 10, 2017; accepted September 3, 2017

E-mail: wf-dce@tsinghua.edu.cn

*These two authors contributed equally to this work.

2 Experimental

SAPO-34 zeolites with different crystal sizes were synthesized following the method reported before [26]. Typically, 11.5 g of AlOOH and 18.5 g of TEOS were added to 50.0 g of deionized water under stirring for 30 min, and then trimethylamine (TEA) was added to the solution. The mixture was transferred into a polytetrafluoroethylene autoclave for hydrothermal crystallization at 200 °C for 48 h under stirring. The amount of AlOOH was changed according to the Si/Al ratio. Polyethylene

glycol (PEG) was used to facilitate the formation of the hierarchical structure as shown in Fig. 1(D). The mole ratio of PEG to TEA was reported in our previous work [26].

The particle size distribution was determined by a laser particle size analyzer (Malvern Instruments Micro-Plus). The range of particle sizes tested was from 0.05 μm to 555 μm. XRD was measured on a Bruker D8 Advance X-ray powder diffractometer to obtain the morphology of SAPO-34 zeolites.

Figure 1 shows the basic information for SAPO-34 zeolites. Zeolites in Figs. 1(A−C) show a perfect cubic morphology. Figure 1 and XRD data in Fig. S1 indicate that all of the four zeolites have the structure of CHA/AEI. Considering that there are no difference in channel diameter between CHA and AEI, the four zeolites can be considered as a proper model catalyst for diffusion measurement.

The equipment for diffusion measurement is exhibited in Fig. 2. The measurement procedure includes three operations: (1) fill the gas into the gas supply and storage chambers, (2) disconnect the two chambers, and (3) open the sample chamber and the gas supply between the connections. After these operations, the sample begins to adsorb the gas. With the adsorption of the sample, the pressure in the gas supply chamber is reduced to a certain extent, and the difference between the supply gas chamber and the gas storage chamber can be measured to obtain the amount of adsorbed gas on the catalyst. This method transforms the traditional mass measurement into a pressure measurement and greatly improves the accuracy of the measurement.

While referring to the coked catalyst, reaction condition was kept at 450 °C and 8 h^{-1} of weight hourly space velocity. After a specific amount of carbon had been

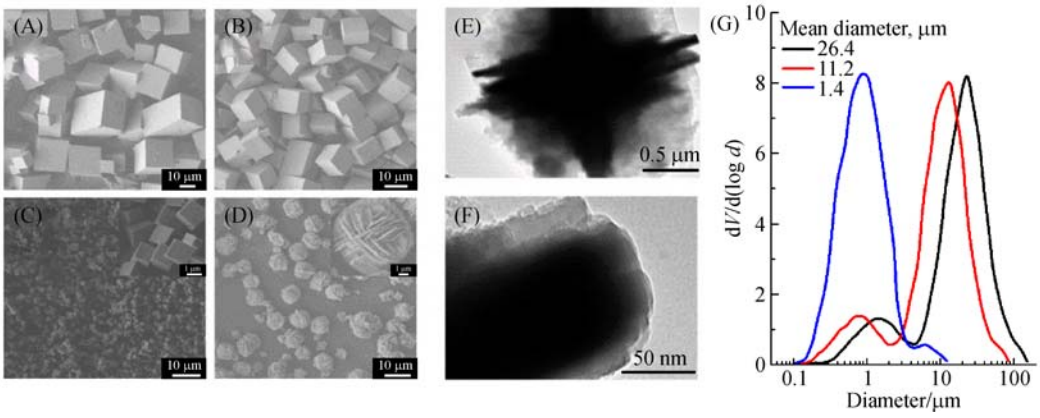

Fig. 1 Characterization of SAPO-34 zeolites with different crystal diameters. SEM images of (A) d_m = 26.4 μm, (B) d_m = 11.2 μm, (C) d_m = 1.4 μm, and (D) SAPO-34 with hierarchical structures (d_{eq} = 0.2 μm); TEM images of (D) on a scale of (E) 0.5 μm and (F) 50 nm; and (G) the diameter distribution from (A) to (C)

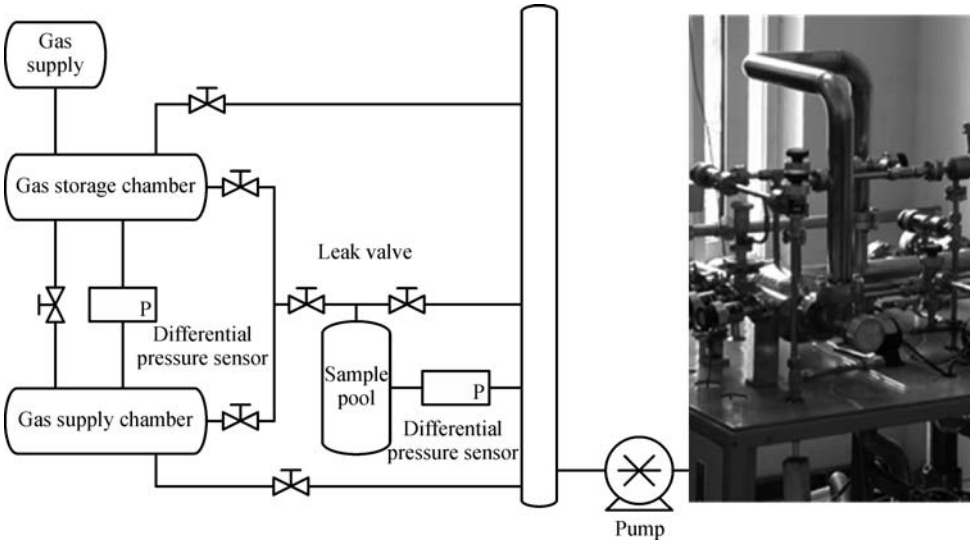

Fig. 2 Flow diagram and physical map of the equipment designed for the high-precision diffusion measurement. Adsorption amount is converted into pressure difference, measured with sensitive differential pressure sensor

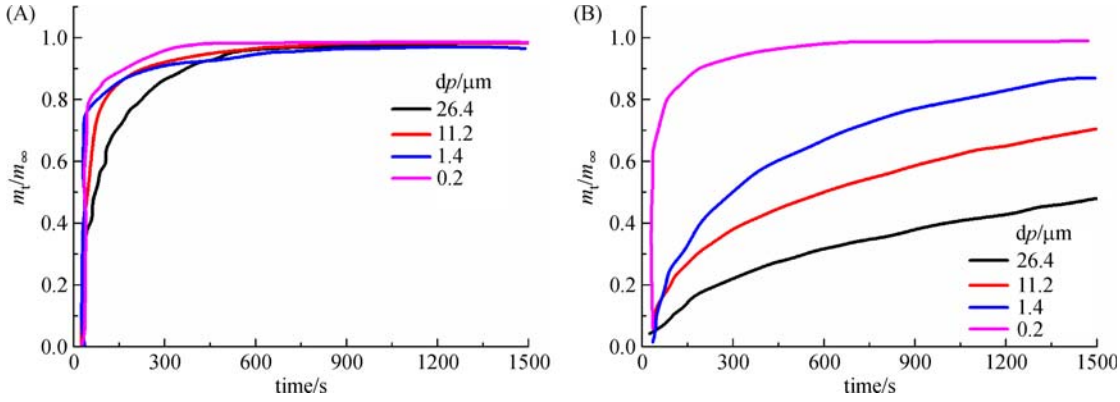

Fig. 3 Adsorption amount *vs.* time with the adsorbents being (A) ethane, and (B) propane on SAPO-34 zeolites

reached, the diffusion behavior on the molecular sieve was measured.

3 Results and discussion

Figure 3 gives the result of diffusion measurement. Figure 3(A) indicates that ethane adsorption reach the equilibrium faster than propane adsorption over all four catalysts. The diffusion rate of ethane shows no difference in SAPO-34 zeolites with different crystal sizes. However, Fig. 3(B) shows that propane diffusion is greatly controlled by the crystal size. The adsorption equilibrium could not be reached even after 1500 s for SAPO-34 zeolites with crystal sizes greater than 0.2 μm, indicating that a bigger crystal has a higher diffusion resistance.

Diffusion of the two molecules were also tested over two typical zeolites at different coke states. Figure 4 shows the diffusion velocity change with coke percentage in zeolite crystals, indicating the coking influence on diffusion. Crystal size shows no effect on diffusion velocity of ethane at different coke percentage, but significant effect on that of propane. Results on coked catalysts are the same as on fresh ones. With the coke percentage rises, the diffusion velocity decreases for all four zeolites. The coke deposition in crystals blocks the diffusion of small molecules, which is a common phenomenon of a zeolite system. However, the deposition of coke shows its higher impact on a bigger molecule. For two different sizes of molecular sieves, the diffusion velocity of propane decreases by an order of magnitude, but that of ethane decreases slightly. Under the reaction condition, the selective resistance to diffusion would further lead to secondary reactions of macromolecules and an increase in carbon deposition. Under this consideration, decreasing the crystal size of SAPO-34 can enhance the diffusion and lower the coking rate.

Based on this, we calculated the diffusion coefficients of different molecules. Considering a zeolite crystal as a sphere, and the influences of external diffusion and surface diffusion can be ignored, we can derive the relationship between experiment and diffusion coefficients as follows:

$$\frac{m_t}{m_\infty} = 1 - \frac{6}{\pi^2}\sum\nolimits_{n=1}^{\infty}\frac{1}{n^2}\exp\left(-\frac{n^2\pi^2 D_c t}{r_p^2}\right),$$

where m_∞ represents the final absorb amount, m_t absorb amount at certain time t, D_c the diffusion coefficient, r_p the particle size. Diffusion coefficients are listed in Table 1.

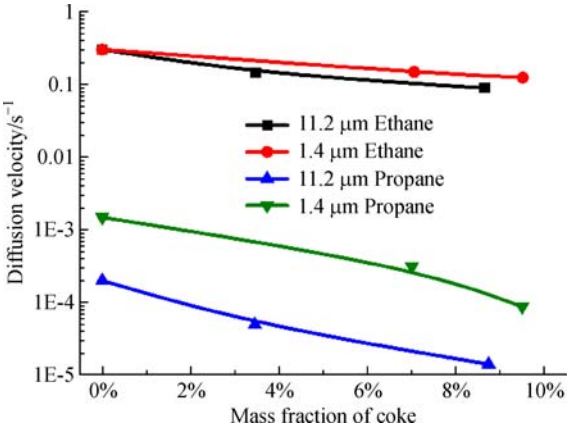

Fig. 4 Diffusion velocity *vs.* coke percentage. The diffusion velocity is defined as the reciprocal of the time at which the diffusion reaches 99% of the equilibrium. Coke mass percentage was measured with TG-DSC

Table 1 Diffusion coefficients of propane and ethane in SAPO-34 zeolites with different diameters

Diameter /μm	D_c (Propane) / ($10^{-15}\cdot m^2\cdot s^{-1}$)	D_c (Ethane) / ($10^{-15}\cdot m^2\cdot s^{-1}$)
26.4	11.97	299.20
11.2	6.24	92.93
1.4	0.19	2.15
0.2	0.04	0.04

The deviation of diffusion coefficient calculated over SAPO-34 zeolites with different diameters cannot be ignored. When deriving the theoretical model, an important hypothesis was made that the external diffusion and surface diffusion were ignored. In our experiment, effect of external diffusion can easily be prevented, but the effect of surface diffusion, which could be a property of catalyst, cannot be prevented by changing the conditions. Under this consideration, a surface resistance may exist in diffusion over SAPO-34 zeolites.

When regarding surface resistance as the main resistance of diffusion in a zeolite system, the relationship between diffusion coefficient and diameter can be derived as follows:

$$\ln\left(1-\frac{m_t}{m_\infty}\right)=-\frac{3Kk_c t}{r_p},$$

where Kk_c represents the surface diffusion coefficient, and other symbol has the same meaning as mentioned above.

With a linear regression, we can calculate the surface diffusion coefficient Kk_c and the results are listed in Table 2. Two different routes for diffusion modeling are compared in Fig. 5. Compared with ethane, propane has a smaller deviation of the surface diffusion coefficient, indicating that the surface diffusion plays a more important role in the diffusion of propane. For ethane, the surface diffusion model shows smaller errors than the model above, but some deviations are also noticed. In this context, the diffusion of ethane cannot be described by only one model, either the surface diffusion model or the traditional internal diffusion model, but the former is more persuasive for both propane and ethane, in general.

Table 2 Surface diffusion coefficient

Diameter /μm	Kk_c (Propane) / $(10^{-10}\cdot m\cdot s^{-1})$	Kk_c (Ethane) / $(10^{-10}\cdot m\cdot s^{-1})$
26.4	43.71	329.81
11.2	34.40	144.70
1.4	7.26	15.41
0.2	3.26	2.84

As reported before [26], the propylene selectivity for small zeolite particles (45%) is higher than big ones (39%). A diffusion-based explanation can be given. For small crystals, the diffusion resistance is greatly reduced for propylene but slightly reduced for ethylene, resulting in a selectivity difference.

From a traditional view of reaction engineering, Thiele modulus and efficiency of different zeolites can be calculated based on the diffusion measurement [27,28]. Nano-sized zeolites and zeolites with a hierarchical structure have a higher efficiency due to their lower diffusion resistance.

Figure 6 gives the Thiele modulus calculated from the diffusion of propane. For big molecules, propane for instance, the diffusion is greatly influenced by its crystal size, and thus Thiele modulus changes. However, Thiele modulus calculated based on ethane does not change with crystal size and the efficiency η keeps at 1. Under this consideration, the selectivity change of ethylene and propylene over time can be reasoned from the aspect of diffusion. As the reaction continues, the coke continues to form but the effect of carbon deposition on the diffusion of ethylene and propylene is different. The diffusion of ethylene is not affected by the coke deposition, whereas that of propylene is. In this way, propylene tends to other reaction pathways like a hydrogen transfer reaction. And that is the reason why the propylene selectivity increases but the ethylene selectivity decreases over time [12].

In conclusion, the diffusion velocity of ethane and propane in SAPO-34 zeolites were measured with the special designed equipment and high-precision results were obtained. The diffusion velocity of ethane shows little relevance with the crystal size of SAPO-34 zeolites and

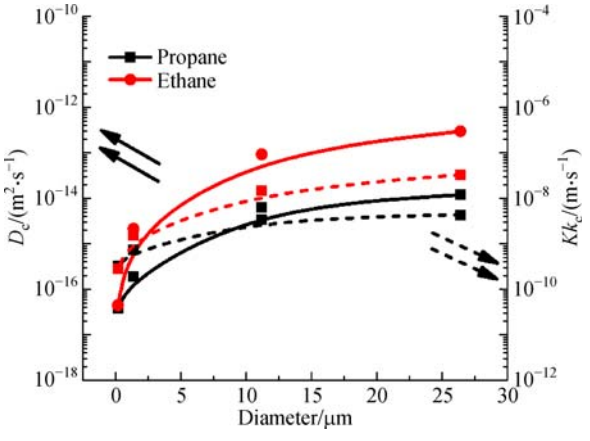

Fig. 5 Relationship between diffusion coefficient and diameter, from traditional diffusion theory (left) and from surface diffusion theory (right)

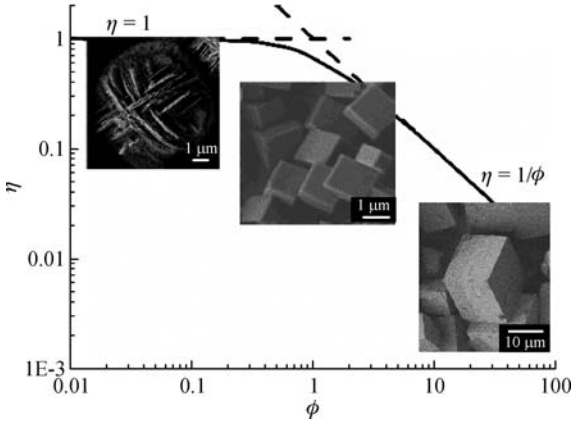

Fig. 6 Several SAPO-34 molecular sieves with different Thiele modulus and efficiency. Calculation is based on propane

with the coke percentage, which in contrast strongly affect the diffusion velocity of propane. With the coke deposition accumulating, the diffusion velocity of propane is drastically reduced. The diffusions of propane and ethane are strongly restricted by the surface diffusion instead of the internal diffusion. The surface diffusion model is effective on describing propane diffusion, whereas the ethane diffusion is more complicated and cannot be perfectly fit by either the surface or internal diffusion model. This work may bring new and quantitative view for MTO study over SAPO-34 zeolites. Further research will be performed to calculate the combination of both the internal and surface diffusion coefficients.

References

1. Su D S, Wen G, Wu S, Peng F, Schlögl R. Carbocatalysis in liquid-phase reactions. Angewandte Chemie International Edition, 2017, 56(4): 936–964
2. Losch P, Pinar A B, Willinger M G, Soukup K, Chavan S, Vincent B, Pale P, Louis B. H-ZSM-5 zeolite model crystals: Structure-diffusion-activity relationship in methanol-to-olefins catalysis. Journal of Catalysis, 2017, 345: 11–23
3. Liang T, Chen J, Qin Z, Li J, Wang P, Wang S, Wang G, Dong M, Fan W, Wang J. Conversion of methanol to olefins over H-ZSM-5 zeolite: Reaction pathway is related to the framework aluminum siting. ACS Catalysis, 2016, 6(11): 7311–7325
4. Fickel D W, Sabnis K D, Li L, Kulkarni N, Winter L R, Yan B, Chen J G. Chloromethane to olefins over H-SAPO-34: Probing the hydrocarbon pool mechanism. Applied Catalysis A, General, 2016, 527: 146–151
5. Li Y, Zhang M, Wang D, Wei F, Wang Y. Differences in the methanol-to-olefins reaction catalyzed by SAPO-34 with dimethyl ether as reactant. Journal of Catalysis, 2014, 311: 281–287
6. Li J, Wei Y, Liu G, Qi Y, Tian P, Li B, He Y, Liu Z. Comparative study of MTO conversion over SAPO-34, H-ZSM-5 and H-ZSM-22: Correlating catalytic performance and reaction mechanism to zeolite topology. Catalysis Today, 2011, 171(1): 221–228
7. Sun X, Mueller S, Shi H, Haller G L, Sanchez-Sanchez M, van Veen A C, Lercher J A. On the impact of co-feeding aromatics and olefins for the methanol-to-olefins reaction on HZSM-5. Journal of Catalysis, 2014, 314: 21–31
8. Sun X, Mueller S, Liu Y, Shi H, Haller G L, Sanchez-Sanchez M, van Veen A C, Lercher J A. On reaction pathways in the conversion of methanol to hydrocarbons on HZSM-5. Journal of Catalysis, 2014, 317: 185–197
9. Ilias S, Bhan A. Mechanism of the catalytic conversion of methanol to hydrocarbons. ACS Catalysis, 2013, 3(1): 18–31
10. Zhou H, Wang Y, Wei F, Wang D, Wang Z. Kinetics of the reactions of the light alkenes over SAPO-34. Applied Catalysis A, General, 2008, 348(1): 135–141
11. Li M, Wang Y, Bai L, Chang N, Nan G, Hu D, Zhang Y, Wei W. Solvent-free synthesis of SAPO-34 nanocrystals with reduced template consumption for methanol-to-olefins process. Applied Catalysis A, General, 2017, 531: 203–211
12. Wu X C, Abraha M G, Anthony R G. Methanol conversion on SAPO-34: Reaction condition for fixed-bed reactor. Applied Catalysis A, General, 2004, 260(1): 63–69
13. Wei Y, Li J, Yuan C, Xu S, Zhou Y, Chen J, Wang Q, Zhang Q, Liu Z. Generation of diamondoid hydrocarbons as confined compounds in SAPO-34 catalyst in the conversion of methanol. Chemical Communications, 2012, 48(25): 3082
14. Li Y, Huang Y, Guo J, Zhang M, Wang D, Wei F, Wang Y. Hierarchical SAPO-34/18 zeolite with low acid site density for converting methanol to olefins. Catalysis Today, 2014, 233: 2–7
15. Wei Z, Chen Y, Li J, Wang P, Jing B, He Y, Dong M, Jiao H, Qin Z, Wang J, et al. Methane formation mechanism in the initial methanol-to-olefins process catalyzed by SAPO-34. Catalysis Science & Technology, 2016, 6(14): 5526–5533
16. Xu S, Zheng A, Wei Y, Chen J, Li J, Chu Y, Zhang M, Wang Q, Zhou Y, Wang J, et al. Direct observation of cyclic carbenium ions and their role in the catalytic cycle of the methanol-to-olefin reaction over chabazite zeolites. Angewandte Chemie International Edition, 2013, 52(44): 11564–11568
17. Qi L, Li J, Wei Y, Xu L, Liu Z. Role of naphthalene during the induction period of methanol conversion on HZSM-5 zeolite. Catalysis Science & Technology, 2016, 6(11): 3737–3744
18. Wei Y, Yuan C, Li J, Xu S, Zhou Y, Chen J, Wang Q, Xu L, Qi Y, Zhang Q, Liu Z. Coke formation and carbon atom economy of methanol-to-olefins reaction. ChemSusChem, 2012, 5(5): 906–912
19. Tian P, Wei Y, Ye M, Liu Z. Methanol to olefins (MTO): From fundamentals to commercialization. ACS Catalysis, 2015, 5(3): 1922–1938
20. Chen D, Rebo H P, Moljord K, Holmen A. Methanol conversion to light olefins over SAPO-34. Sorption, diffusion, and catalytic reactions. Industrial & Engineering Chemistry Research, 1999, 38 (11): 4241–4249
21. Aguayo A T, Del Campo A, Gayubo A G, Tarrio A, Bilbao J. Deactivation by coke of a catalyst based on a SAPO-34 in the transformation of methanol into olefins. Journal of Chemical Technology and Biotechnology (Oxford, Oxfordshire), 1999, 74 (4): 315–321
22. Hwang A, Prieto-Centurion D, Bhan A. Isotopic tracer studies of methanol-to-olefins conversion over HSAPO-34: The role of the olefins-based catalytic cycle. Journal of Catalysis, 2016, 337: 52–56
23. Yang G, Wei Y, Xu S, Chen J, Li J, Liu Z, Yu J, Xu R. Nanosize-enhanced lifetime of SAPO-34 catalysts in methanol-to-olefin reactions. Journal of Physical Chemistry C, 2013, 117(16): 8214–8222
24. Zhu W, Kapteijn F, Moulijn J A, den Exter M C, Jansen J C. Shape selectivity in adsorption on the all-silica DD3R. Langmuir, 2000, 16 (7): 3322–3329
25. Olson D H, Camblor M A, Villaescusa L A, Kuehl G H. Light hydrocarbon sorption properties of pure silica Si-CHA and ITQ-3 and high silica ZSM-58. Microporous and Mesoporous Materials, 2004, 67(1): 27–33
26. Cui Y, Zhang Q, He J, Wang Y, Wei F. Pore-structure-mediated hierarchical SAPO-34: Facile synthesis, tunable nanostructure, and

catalysis applications for the conversion of dimethyl ether into olefins. Particuology, 2013, 11(4): 468–474

27. Bhatia S K, Perlmutter D D. A random pore model for fluid-solid reactions: II. Diffusion and transport effects. AIChE Journal. American Institute of Chemical Engineers, 1981, 27(2): 247–254
28. Thiele E W. Relation between catalytic activity and size of particle. Industrial & Engineering Chemistry, 1939, 31(7): 916–920